Quantum nonlinear optics near optomechanical instabilities

Xunnong Xu, Michael Gullans, and Jacob M. Taylor

Quantum Nonlinear Optics Near Optomechanical Instabilities

Xunnong Xu, Michael Gullans, and Jacob M. Taylor
*Joint Quantum Institute, University of Maryland/National Institute
of Standards and Technology, College Park, Maryland 20742, USA*
(Dated: December 17, 2014)

Optomechanical systems provide a unique platform for observing quantum behavior of macroscopic objects. However, efforts towards realizing nonlinear behavior at the single photon level have been inhibited by the small size of the radiation pressure interaction. Here we show that it is not necessary to reach the single-photon strong-coupling regime in order to realize significant optomechanical nonlinearities. Instead, nonlinearities at the few quanta level can be achieved, even with weak-coupling, in a two-mode optomechanical system driven near instability. In this limit, we establish a new figure of merit for realizing strong nonlinearity which scales with the single-photon optomechanical coupling and the sideband resolution of the mechanical mode with respect to the cavity linewidth. We find that current devices based on optomechanical crystals, thought to be in the weak-coupling regime, may be able to achieve strong quantum nonlinearity; enabling deterministic interactions between single photons.

I. INTRODUCTION

Recent years have seen dramatic progress in realizing deterministic interactions between single photons, which has profound implications for future optical technologies [1–4]. The most striking success has been achieved with cavity quantum electrodynamics (cQED) [5–12], where photons inherent the saturation of a single two-level atom due to strong interactions between the atom and the cavity field. Alternative approaches have been explored based on slow-light-enhanced Kerr nonlinearites [13–15], single dye-molecules [16], strong photon interactions mediated by Rydberg atoms [17–20], enhanced nonlinearities in plasmonic systems [21, 22] and atoms coupled to wave guides[23–26].

Optomechanical systems, where light and mechanical motion are coupled by radiation pressure [27–33], are a promising approach to realizing strong photon interactions. Unfortunately no experiment has yet managed to reach the single-photon strong coupling regime. Recently it was noted that, in the weak coupling regime, there are still signatures of optomechanical nonlinearity [34–36]; however, strong coupling is required to achieve significant nonlinear quantum effects and deterministic photon interactions with optomechanics [37–40].

In this article, we show that it may not be necessary to reach the quantum strong coupling regime in order to obtain large single-photon nonlinearities. Instead, in two-mode optomechanical systems with strong side-band resolution, the nonlinearity can be enhanced to the single-photon level by driving the system near an instability. In particular, as the strength of the driving field increases, the frequency of one of the optomechanical normal modes approaches zero and the associated harmonic oscillator length becomes large [41]. The increased quantum fluctuations associated with this mode result in an enhanced nonlinear interaction. We show that when the mechanical mode is sideband resolved with respect to the cavity, the enhancement in the nonlinear coupling can exceed the dissipation by an amount scaling with the sideband resolution ω_m/κ, where ω_m is the mechanical frequency and κ is the cavity linewidth. We demonstrate that this results in enhanced photon-photon interactions by calculating the equal time, two-photon correlation function $g^{(2)}(0)$ for weakly incident probe light. The presence of anti-bunching $g^{(2)}(0) < 1$ in the cavity output field indicates the onset of photon blockade and, in this case, significant two-photon nonlinearity. We infer a new parameter $P = g_0^2\omega_m/\kappa^3$ (g_0 is single-photon optomechanical coupling), whose largeness is the relevant quantity for determining the strength of the nonlinearity. We find that in current devices based on optomechanical crystals, our approach could increase the observable antibunching by more than an order of magnitude.

In section II, we describe the system using an effective hamiltonian and show that after diagonalization, the nonlinear interaction is strongly enhanced. In section III, we take dissipation into account using the master equation and determine the conditions for realizing strong quantum nonlinearity. Subsequently, in section IV, we discuss the photon-blockade mechanism and present numerical simulations for the two-photon correlation functions. In section V, we discuss the feasibilities of our scheme and do a case study in optomechanical crystals.

II. MODEL

The system we consider is shown in Fig. 1(a). It consists of a high finesse optical cavity that has two spatially separated, degenerate optical modes (a_L, a_R) at frequency ω_c coupled at a rate J through a mirror with near perfect reflection [42]. Both optical modes are also coupled to a common mechanical mode (c) through radiation pressure with single-photon optomechanical coupling rate g_0. In the symmetric-antisymmetric mode ba-
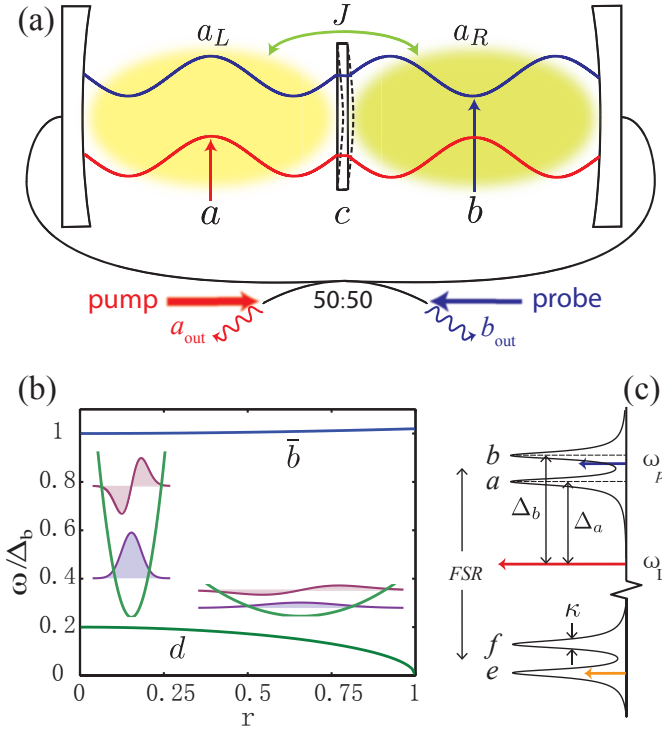
FIG. 1. (color online). (a) Schematic of the coupled two-mode system. Displacements of the middle mirror (via mechanical oscillations) couple the symmetric mode a (red) and antisymmetric mode b (blue) as the left-right symmetry is broken. (b) Normal modes of the coupled harmonic oscillator bilinear hamiltonian for $\Delta_b = 5\omega_m$, with blue (green) line representing the higher (lower) energy branch $\bar{b}$ (d). As pump power increases, the energy of the lower branch decreases, the effective potential becomes flat and the associated harmonic oscillator length becomes larger. (c) Energy scales for the pump, probe and cooling modes.

sis $a = (a_L + a_R)/\sqrt{2}$, $b = (a_L - a_R)/\sqrt{2}$ the Hamiltonian is ($\hbar = 1$):

$$H = (\omega_c - J)a^\dagger a + (\omega_c + J)b^\dagger b + \omega_m c^\dagger c$$
$$- g_0(a^\dagger b + b^\dagger a)(c + c^\dagger) . \tag{1}$$

In addition, there is also a dissipative interaction of the cavity and mechanical modes with their environment, with a conservative term $V = \sqrt{\kappa}(a_{\rm in}(t)a^\dagger + h.c.)$ and damping κ (described below). The two cavities are assumed to have identical damping rates.

In the presence of a strong drive $a_{\rm in}(t) = a_{\rm in} + \sqrt{\kappa}\,\alpha_{\rm p}e^{-i\omega t}$ there is an an effective linear coupling between the antisymmetric mode and the mechanical mode, and also a residual nonlinear coupling between the mechanical mode and both optical modes. The Hamiltonian in the rotating frame for the pump displaced oscillator

states ($a \to a + \alpha$) becomes [28]

$$H = \Delta_a a^\dagger a + \Delta_b b^\dagger b + \omega_m c^\dagger c - G_0(b + b^\dagger)(c + c^\dagger)$$
$$- g_0(a^\dagger b + b^\dagger a)(c + c^\dagger) \tag{2}$$

where $\Delta_{a(b)}$ is the detuning of mode a (b) with respect to the pumping laser and $G_0 \equiv g_0\alpha = g_0\alpha_p\kappa/(\Delta_a - i\kappa/2)$ is the pump-enhanced linear coupling. By choosing an appropriate phase of the pump, we can make G_0 real. In what follows, we make the further assumptions that $\Delta_b \gg \omega_M$, such that the parameter $\eta \equiv \omega_m/\Delta_b$ is much smaller than 1. In this regime the hybridized polariton modes Eq. (4)-(5) retain mostly their original photonic or mechanical character, reducing the deleterious effect of optical loss on the 'mechanical' mode. We give the full expressions in Appendix A and Appendix B.

The first four terms in H are bilinear in the oscillator modes and can be diagonalized to give the normal modes (see Appendix A)

$$H_0 = \Delta_a a^\dagger a + (\Delta_b + \delta)\bar{b}^\dagger \bar{b} + \omega_m \zeta \, d^\dagger d, \tag{3}$$

with the normal mode frequencies given in terms of the parameters $\delta \approx r^2\omega_m\eta/2$ and $\zeta = \sqrt{1 - r^2}$ to first order in η. We defined the rescaled driving amplitude $r \equiv 2G_0/\sqrt{\omega_m\Delta_b}$. As $r \to 1$ the frequency of the lower branch goes to zero and the mode effectively becomes a free particle, leading to enhanced quantum fluctuations in this mode, as shown in Fig. 1(b). For $r > 1$, the normal mode frequency becomes imaginary signifying the onset of the instability. For $0 \le r < 1$ and $\eta \ll 1$, the normal mode operators are, surprisingly

$$\bar{b} \approx b - \frac{r}{2}\sqrt{\eta}(c + c^\dagger), \tag{4}$$

$$d \approx \frac{1}{2\sqrt{\zeta}}(c - c^\dagger) + \frac{\sqrt{\zeta}}{2}(c + c^\dagger) + \frac{r}{2}\sqrt{\eta}(b - b^\dagger). \tag{5}$$

In this regime, $\bar{b}$ is mostly optical while d is mostly mechanical, to $O(r\sqrt{\eta})$. Including the nonlinearity, we can reexpress the normal-ordered Hamiltonian to first order in η

$$H = H_0 - \frac{g_0}{\sqrt{\zeta}}(a^\dagger\bar{b} + a\bar{b}^\dagger)(d + d^\dagger) \tag{6}$$
$$- \frac{g_0}{\sqrt{\zeta}}\sqrt{\frac{\eta}{4\zeta}}(a + a^\dagger)(d^2 + d^{\dagger 2} + 2d^\dagger d).$$

Near the instability, $\zeta \ll 1$, the effective optomechanical coupling $g_0/\sqrt{\zeta}$ is strongly enhanced. This approach is distinct from simply choosing a low frequency mechanical oscillator to begin with because the mass and frequency of a mechanical oscillator (of the same shape and material) are usually related to each other by $\omega_m \propto \sqrt{1/m}$, so that the stiffness $m\omega_m^2$ remains constant. As a result, the optomechanical coupling g_0, which scales with the intrinsic position fluctuations $x_{\rm zpf} = \sqrt{\hbar/m\omega_m}$, will typically increase with frequency. This back-action induced softening has the benefits of combining small mass and low frequency, so the effective coupling can be enhanced substantially.

III. NONLINEAR INTERACTIONS AND DISSIPATIONS

In the normal mode basis, H contains five distinct nonlinear interactions:

$$\bar{b}^{\dagger}ad + h.c., \quad a^{\dagger}\bar{b}d + h.c., \quad a^{\dagger}dd + h.c.,$$
$$add + h.c., \quad (a + a^{\dagger})d^{\dagger}d. \tag{7}$$

When the frequency of the d mode is small, these nonlinear terms will destabilize the system towards large mode occupation, which, together, with the cavity induced decay will contaminate any few photon effects. To keep the system far in the stable regime, we require $g_0/\sqrt{\zeta}, g_0\sqrt{\eta/\zeta^2} \ll \omega_m\zeta$, which further constrains Δ_b and ζ. In addition, the mechanical mode must be close to the ground state, below we show how this can be achieved with optomechanical cooling for the normal mode when the heating rate $\gamma_{\uparrow}$ (defined below) is much less than κ. All together, to have a large effective single photon optomechanical nonlinearity we require

$$\gamma_{\uparrow} \ll \kappa \ll g_0/\sqrt{\zeta} \ll \omega_m\zeta. \tag{8}$$

This can be satisfied for large Δ_b and small $\gamma_{\uparrow}$ when

$$P \equiv \frac{g_0^2}{\kappa^2}\frac{\omega_m}{\kappa} \gg 1. \tag{9}$$

Thus the condition for single photon nonlinearities is relaxed from $g_0 \gg \kappa$ to $P \gg 1$.

To treat the dissipation we use the master equation for the density matrix ρ of the three-mode system

$$\dot{\rho} = -i[H, \rho] - \kappa\big(\mathcal{D}[a] + \mathcal{D}[b]\big)\rho$$
$$- \gamma_m\big((\bar{n}_{\text{th}} + 1)\mathcal{D}[c] + \bar{n}_{\text{th}}\mathcal{D}[c^{\dagger}]\big)\big)\rho, \tag{10}$$

where $\mathcal{D}[A]\rho = 1/2\{A^{\dagger}A, \rho\} - A\rho A^{\dagger}$ for any operator A, γ_m is the mechanical heating rate, and $\bar{n}_{\text{th}}$ is the thermal occupation of the mechanical mode in the absence of the coupling to the cavity. In the normal mode basis, the jump operator for the cavity and mechanical modes become $b \to \bar{b} + \sqrt{\eta/\zeta}\,(d + d^{\dagger})/2$ and $c \to (d + d^{\dagger})/2\sqrt{\zeta} + \sqrt{\zeta}(d - d^{\dagger})/2$, respectively, implying that dissipation of both cavity mode b and mechanical mode c results in added noise on the d mode. Near the instability $\zeta \ll 1$, the downward transitions (emission) and upward transitions (absorption) in the d mode occur at the respective rates

$$\gamma_{\downarrow} = \frac{\eta}{4\zeta}\kappa + \frac{\gamma_m}{4\zeta}(2\bar{n}_{\text{th}} + 1 + 2\zeta), \tag{11}$$

$$\gamma_{\uparrow} = \frac{\eta}{4\zeta}\kappa + \frac{\gamma_m}{4\zeta}(2\bar{n}_{\text{th}} + 1 - 2\zeta). \tag{12}$$

Since $\gamma_{\downarrow} - \gamma_{\uparrow} = \gamma_m \ll \gamma_{\uparrow}$, the absorption terms will tend to excite the d mode to high occupation numbers roughly given by $\bar{n}_d \sim \gamma_{\uparrow}/(\gamma_{\downarrow} - \gamma_{\uparrow})$ [28].

A natural way to overcome this difficulty is to add optomechanical cooling to the d mode. As shown in
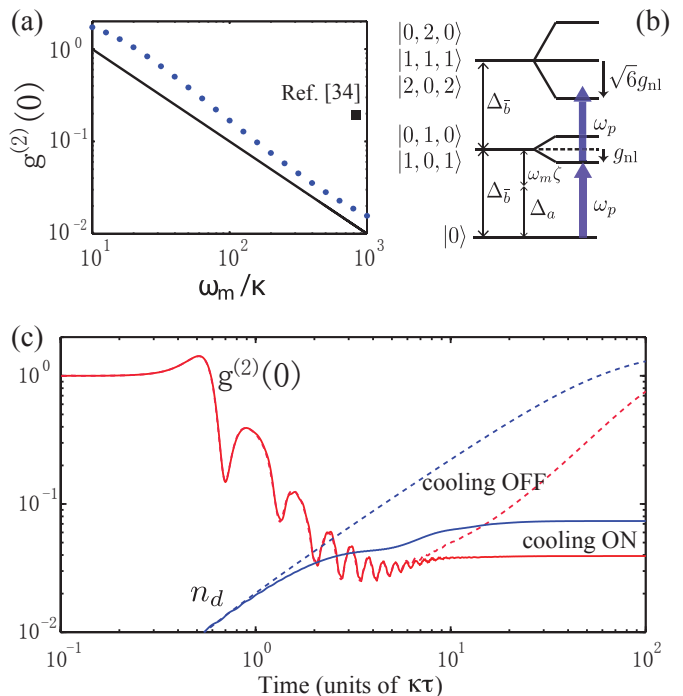

FIG. 2. (color online). (a) Dotted line shows $g^2(0)$ of the $\bar{b}$ mode as a function of P with $g_0 = \kappa$ (so $P = \omega_m/\kappa$), $\alpha_e = 0.1$ and $\beta_{\bar{b}} = 0.02\kappa$. We restrict the mode occupations to be less than 4. When $P > 40$, $g^2(0)$ roughly scales as $1/P$ (black line). The black square represents the value of $g^2(0)$ obtained in Ref. [34] when $\omega_m/\kappa \to \infty$. For comparison, the $g^2(0)$ in Ref. [37], when $g_0 = \kappa$, increases linearly with P^2. (b)The level diagram of the system when the interaction $\bar{b}^{\dagger}ad$ becomes resonant. The probe field drives the lower energy state of the first excited state on resonance. (c) Evolution of the equal time, two-photon correlation function $g^{(2)}(0)$ (red lines) and the population in the d mode $n_d = \langle d^{\dagger}d \rangle$ (blue lines), after the probe field is turned on ($P = 500$, $g_0 = \kappa$, $\gamma_{\uparrow\downarrow} = \kappa/\sqrt{P}$ and $\beta_{\bar{b}} = 0.02\kappa$). Dotted lines show the result for $\alpha_e = 0$ indicating cooling on d is OFF, while solid lines are for $\alpha_e = 0.1$ indicating cooling is ON.

Fig. 1(c), we consider using another pair of cavity modes e, f separated by the cavity free spectrum range (FSR) to induce sideband cooling of the d mode. Driving mode e enhances the coupling between mode f and the mechanical mode c by an amount α_e, the steady state amplitude of e. Moving to the optomechanical normal mode basis, we get the additional terms in the hamiltonian:

$$\Delta_e e^{\dagger}e + \Delta_f f^{\dagger}f - \frac{g_0}{\sqrt{\zeta}}\alpha_e(f + f^{\dagger})(d + d^{\dagger}). \tag{13}$$

We see that the coupling is further enhanced by $1/\sqrt{\zeta}$ because of the increase of harmonic oscillator length. Similar to the usual single-mode optomechanical cooling, when $\Delta_f = \omega_m\zeta$, the d mode is cooled by the f mode [28] and the system quickly reaches steady state.

IV. PHOTON-BLOCKADE AND NUMERICAL SIMULATIONS OF $g^2(0)$

The nonlinear terms will have the strongest effect when one of the interactions in Eq. (7) is tuned into resonance. Here we focus on the resonant interaction $\bar{b}^\dagger ad$, which has the resonance condition: $\Delta_{\bar{b}} = \Delta_a + \omega_m \zeta$ (Here $\Delta_{\bar{b}} = \Delta_b + \delta$ is the energy of the normal mode $\bar{b}$). In the occupation number basis $|n_a, n_{\bar{b}}, n_d\rangle$, the 2-fold degeneracy of the first excited state is broken by $g_{\rm nl}$ and the 3-fold degeneracy of the second excited state is broken by $\sqrt{6}g_{\rm nl}$ due to the 3-body interaction $\bar{b}^\dagger ad + $ h.c.:

$$|0,1,0\rangle \xleftrightarrow{g_{\rm nl}} |1,0,1\rangle, \ \Delta\omega : \pm g_{\rm nl}$$

$$|0,2,0\rangle \xleftrightarrow{\sqrt{2}g_{\rm nl}} |1,1,1\rangle \xleftrightarrow{2g_{\rm nl}} |2,0,2\rangle, \ \Delta\omega : 0, \pm\sqrt{6}g_{\rm nl}$$

with $g_{\rm nl} = g_0/\sqrt{\zeta}$. Since $\bar{b}$ has a strong overlap with the antisymmetric cavity mode, we can optically probe it as illustrated in Fig. 1. Similar to the Jaynes-Cummings nonlinearity in cQED system [5], when probing the $\bar{b}$ mode at frequency $\omega_p = \Delta_{\bar{b}} - g_{\rm nl}$ with strength $\beta_{\bar{b}}$, we can observe a photon-blockade effect because of the anharmonicity of the ladders, which is shown in Fig. 2(b). The signature of the photon blockade will be in the antibunching of the output light, i.e., when $g^{(2)}(0) < 1$, where $g^{(2)}(0)$ is the equal time, two-photon correlation function defined by

$$g^{(2)}(t) = \frac{\langle \bar{b}^\dagger(\tau)\bar{b}^\dagger(\tau+t)\bar{b}(\tau+t)\bar{b}(\tau)\rangle}{\langle \bar{b}^\dagger(\tau)\bar{b}(\tau)\rangle^2} \quad (14)$$

for a given evolution time τ. Fig. 2(a) shows that, for optimal parameters described below, the minimum value of $g^{(2)}(0) \sim 1/P$, thus the system exhibits a strong single photon nonlinearity even when $g_0 \lesssim \kappa$.

Fig. 2(c) shows the typical evolution of $g^{(2)}(0)$ with τ obtained from numerical simulation of the master equation. The initial condition has all modes in the vacuum state. Without cooling the system reaches a quasi-steady state with strong antibunching before it is eventually pumped to states with a finite population in d as shown by the dashed blue line in Fig. 2(c). However, in the presence of cooling the d mode occupation remains small and the system reaches a steady state with strong antibunching.

To achieve single photon blockade using the scheme illustrated in Fig. 2(b), we also need to satisfy the inequalities given in Eq. (8), which requires optimization of the system parameters. After rescaling by κ and taking the resonance condition $\Delta_{\bar{b}} = \Delta_a + \omega_m \zeta$, there are four independent parameters: $(P, \omega_m/\kappa, \Delta_{\bar{b}}/\kappa, \zeta)$. P and ω_m/κ are device-dependent parameters we cannot tune, while $\Delta_{\bar{b}}/\kappa$ and ζ can be controlled by tuning the frequency and amplitude of the strong pumping laser. A simple theoretical analysis can be done for $\beta_{\bar{b}} \ll \kappa$ by neglecting quantum jumps in the master equation (see Appendix C for details). This gives the scaling in the quasi-steady
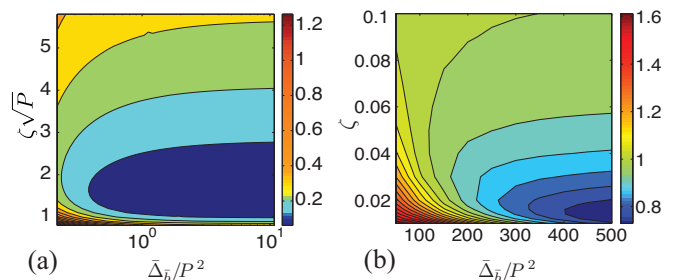

FIG. 3. (color online). Contour plots of the minimum $g^{(2)}(0)$ in steady state versus the experimental control parameters $\bar{\Delta}_{\bar{b}} = \Delta_{\bar{b}}/\kappa$ and ζ. (a) $P = 100$, $\omega_m/\kappa = P$; (b) $g_0/\kappa = 0.1$, $\omega_m/\kappa = 500$, $P = 5$ and $\alpha_e = 2\sqrt{\zeta}$.

state regime $g^2(0) \sim \kappa^2/g_{\rm nl}^2 + g_{\rm nl}^2/\omega_m^2\zeta^2$, which is optimized when $\zeta \sim 1/\sqrt{P}$ and $g^{(2)}(0) \sim 1/\sqrt{P}$. Numerical simulations of the master equation however, show that the optimal antibunching scales as $1/P$, as seen in Fig. 2(a) and in the full contour plots of $g^{(2)}(0)$ versus $\Delta_{\bar{b}}$ and ζ shown in Fig. 3. This anomalous scaling is caused by pumping into the dark states $|0,0,n\rangle$. The region of the parameter space for optimal performance is roughly given by $\Delta_{\bar{b}}/\kappa > P^2$ and $1/\sqrt{P} < \zeta < 1$. These results demonstrate that near the instability, the figure of merit for observing the photon blockade is $P \gg 1$ and not simply $g_0/\kappa \gg 1$.

V. EXPERIMENTAL CONSIDERATIONS AND CASE STUDY

There is an additional constraint that, in order to use the resonant $\bar{b}^\dagger ad$ interaction term, the photon tunneling rate J must be much smaller than the mechanical frequency ω_m. For the membrane in the middle setup, these conditions may be challenging to achieve due to the high reflectivity required for the membrane. This could be circumvented by instead utilizing the $a^\dagger dd$ nonlinearity, which has no such requirement. One can also consider using differential modes in 'zipper' optomechanical crystals [44], where the photon tunneling rate can be tuned over a wide range by controlling the separation between the two cavities.

Finally, successfully working near the instability requires the classical power fluctuations in the pump laser to be small enough to prevent the system from crossing the instability. More precisely, the amplitude fluctuations in the pump must be less than the instability parameter ζ (defined below Eq. (3)), which has an optimum value greater than $1/\sqrt{P}$; thus, for P less than 10^3, this requires stabilizing the pump power below the 5 % level, which is readily achievable.

Case study – Experimentally these effects could be observed for systems with strong sideband resolution $\omega_m \gg \kappa$ and relatively large single photon optomechan-

ical coupling $g_0 \sim \kappa$. Hybrid photonic-phononic crystals are a promising route to realize both these constraints [30], as are mechanical membranes placed in the middle of a high-finesse optical cavity as illustrated in Fig. 1(a) [29]. State of the art photonic-phononic crystals have achieved optomechanical coupling $g_0/2\pi$ above 1 MHz [45, 46] and mechanical frequency $\omega_m/2\pi \sim 10$ GHz [47]. Optical quality factors as high as nine million have also been reported in silicon photonic crystal cavities, which gives cavity decay rate of $\kappa/2\pi \sim 20$ MHz [48]. In such a case with $g_0/\kappa = 0.1$ and $\omega_m/\kappa = 500$, P can be as large as 5 in current devices. Fig. 3(b) shows the full range of antibunching obtainable for this P, in the optimal case we find that it can be as small as 0.8, more than an order of magnitude improvement compared to what would be expected away from the instability ~ 0.99 [35]. To satisfy the condition $\gamma_\uparrow \ll \kappa$, we need $\omega_m/4\zeta\Delta_b \ll 1$ and $\gamma_m \bar{n}_{\rm th}/2\zeta \ll \kappa$, which imply $\Delta_b \gg \omega_m/4\zeta$ and $\bar{n}_{\rm th} \ll 2\zeta\kappa/\gamma_m$. This gives an minimum requirement on the Q·frequency product: $Q_m \cdot \omega_m/2\pi > \omega_m/2\zeta\kappa \cdot k_B T/h$, which requires cryogenic temperatures. In principle, room temperature operation is possible for mechanical oscillators at frequencies above 10 GHz and quality factors above 10^6.

VI. CONCLUSION

We have presented a scheme to realize few-photon interactions in strongly driven, two-mode optomechanical systems. Our approach suggests a new figure of merit for realizing strong optomechanical coupling and demonstrates that current devices, previously thought to have weak coupling, may be able to be pushed into the regime of strong single-photon nonlinearity. This would allow one to achieve deterministic entanglement of light in optomechanical systems, which has far-ranging applications in quantum information science.

VII. ACKNOWLEDGEMENTS

Appendix A: Diagonalization of the bilinear hamiltonian

The bilinear hamiltonian in the first line of Eq. (2) is

$$H_0 = \Delta_a a^\dagger a + \Delta_b b^\dagger b + \omega_m c^\dagger c - G_0(b + b^\dagger)(c^\dagger + c). \tag{A1}$$

In this hamiltonian, mode a is already decoupled, so we only need to diagonalize the coupled harmonic oscillator subsystem $b - c$. Define the quadrature variables as

$$X_b = (b + b^\dagger)/\sqrt{2}, \quad Y_b = (b - b^\dagger)/i\sqrt{2}, \tag{A2a}$$

$$X_c = (c + c^\dagger)/\sqrt{2}, \quad Y_c = (c - c^\dagger)/i\sqrt{2}. \tag{A2b}$$

They satisfy the commutation relations $[X_b, Y_b] = [X_c, Y_c] = i$, $[X_b, X_c] = [X_b, Y_c] = [Y_b, X_c] = [Y_b, Y_c] = 0$. We can then rewrite the hamiltonian of the $b - c$ subsystem as

$$H_{bc} = \frac{1}{2}\Delta_b(X_b^2 + Y_b^2) + \frac{1}{2}\omega_m(X_c^2 + Y_c^2) - 2G_0 X_b X_c. \tag{A3}$$

We now rescale the operators X_c and Y_c according to

$$X_c = X_c'\sqrt{\omega_m/\Delta_b}, \quad Y_c = Y_c'\sqrt{\Delta_b/\omega_m}, \tag{A4}$$

but keep X_b and Y_b the same

$$X_b = X_b', \quad Y_b = Y_b'. \tag{A5}$$

In this transformed basis the hamiltonian becomes

$$H_{bc} = \frac{1}{2}\Delta_b(X_b'^2 + Y_b'^2) + \frac{1}{2}\Delta_b\left(\frac{\omega_m^2}{\Delta_b^2}X_c'^2 + Y_c'^2\right)$$
$$- 2G_0\sqrt{\frac{\omega_m}{\Delta_b}}X_b'X_c'. \tag{A6}$$

We then make an unitary transformation to get the normal mode coordinates that yields

$$\begin{pmatrix} X_b' \\ X_c' \end{pmatrix} = \begin{pmatrix} \alpha & \beta \\ -\beta & \alpha \end{pmatrix}\begin{pmatrix} X_+ \\ X_- \end{pmatrix}, \tag{A7a}$$

$$\begin{pmatrix} Y_b' \\ Y_c' \end{pmatrix} = \begin{pmatrix} \alpha & \beta \\ -\beta & \alpha \end{pmatrix}\begin{pmatrix} Y_+ \\ Y_- \end{pmatrix}. \tag{A7b}$$

The commutation relations are preserved if $\alpha^2 + \beta^2 = 1$ (α, β are real).

So the hamiltonian of the $b - c$ subsystem is given by

$$H_{bc} = \frac{1}{2}\Delta_b\left(\alpha^2 + \frac{\omega_m^2}{\Delta_b^2}\beta^2 + \frac{4G_0}{\Delta_b}\sqrt{\frac{\omega_m}{\Delta_b}}\alpha\beta\right)X_+^2 + \frac{1}{2}\Delta_b\left(\beta^2 + \frac{\omega_m^2}{\Delta_b^2}\alpha^2 - \frac{4G_0}{\Delta_b}\sqrt{\frac{\omega_m}{\Delta_b}}\alpha\beta\right)X_-^2$$
$$+ \frac{1}{2}\Delta_b\left(Y_+^2 + Y_-^2\right) + \left[\frac{1}{2}\Delta_b 2\alpha\beta(1 - \frac{\omega_m^2}{\Delta_b^2}) - 2G_0\sqrt{\frac{\omega_m}{\Delta_b}}(\alpha^2 - \beta^2)\right]X_+X_-. \tag{A8}$$

It is diagonal if the cross term X_+X_- is zero:

$$\Delta_b\alpha\beta(1 - \frac{\omega_m^2}{\Delta_b^2}) - 2G_0\sqrt{\frac{\omega_m}{\Delta_b}}(\alpha^2 - \beta^2) = 0. \tag{A9}$$

This condition along with $\alpha^2 + \beta^2 = 1$ determines α and β for the normal modes. The diagonalized hamiltonian thus becomes

$$H_{bc} = \frac{1}{2}\Delta_b(\xi_+^2 X_+^2 + Y_+^2) + \frac{1}{2}\Delta_b(\xi_-^2 X_-^2 + Y_-^2) \tag{A10}$$

with

$$\xi_+^2 = \alpha^2 + \frac{\omega_m^2}{\Delta_b^2}\beta^2 + \frac{4G_0}{\Delta_b}\sqrt{\frac{\omega_m}{\Delta_b}}\alpha\beta, \tag{A11a}$$

$$\xi_-^2 = \beta^2 + \frac{\omega_m^2}{\Delta_b^2}\alpha^2 - \frac{4G_0}{\Delta_b}\sqrt{\frac{\omega_m}{\Delta_b}}\alpha\beta. \tag{A11b}$$

In the limit described in the main text with $\omega_m \ll \Delta_b$, $\xi_+ \approx 1$ and $\xi_- \approx \eta\zeta$.

The diagonalized hamiltonian describes two decoupled harmonic oscillators HO+ and HO− with effective masses $m_\pm = \Delta_b^{-1}$ and effective frequencies $\omega_\pm = \Delta_b\xi_\pm$, so it can be rewritten as

$$H_{bc} = H_+ + H_- \tag{A12}$$
$$= \frac{Y_+^2}{2\Delta_b^{-1}} + \frac{1}{2}\Delta_b^{-1}(\Delta_b\xi_+)^2 X_+^2$$
$$+ \frac{Y_-^2}{2\Delta_b^{-1}} + \frac{1}{2}\Delta_b^{-1}(\Delta_b\xi_-)^2 X_-^2.$$

We can write the wavefunction of the nth eigenstate of HO− (for example) in position representation:

$$\psi_n(X_-) = \frac{1}{\sqrt{2^n n!}}\left(\frac{\xi_-}{\pi}\right)^{1/4} e^{-\frac{\xi_-}{2}X_-^2} H_n(\sqrt{\xi_-}X_-). \tag{A13}$$

as illustrated in Fig. 1(b) for the ground state ($n = 0$) and the first excited state ($n = 1$) for two values of ξ_-.

Appendix B: Hamiltonian in the normal mode basis

We now focus on the nonlinear interaction term in the hamiltonian (second line of Eq. (2)). We define new squeezed operators

$$d_\pm = \sqrt{\frac{\xi_\pm}{2}}X_\pm + i\sqrt{\frac{1}{2\xi_\pm}}Y_\pm, \tag{B1}$$

so $[d_\pm, d_\pm^\dagger] = 1$, $[d_\pm, d_\mp^\dagger] = 0$, and $\xi_\pm^2 X_\pm^2 + Y_\pm^2 = 2\xi_\pm(d_\pm^\dagger d_\pm + 1)$. The bilinear hamiltonian H_0 written in new operators is

$$H_0 = \Delta_a a^\dagger a + \omega_+ d_+^\dagger d_+ + \omega_- d_-^\dagger d_-. \tag{B2}$$

The new operators written in original operators are:

$$d_+ = \frac{\sqrt{\xi_+}}{2}\left[\alpha(b + b^\dagger) - \beta\sqrt{\frac{\Delta_b}{\omega_m}}(c + c^\dagger)\right] + \frac{1}{2\sqrt{\xi_+}}\left[\alpha(b - b^\dagger) - \beta\sqrt{\frac{\omega_m}{\Delta_b}}(c - c^\dagger)\right], \tag{B3a}$$

$$d_- = \frac{\sqrt{\xi_-}}{2}\left[\beta(b + b^\dagger) + \alpha\sqrt{\frac{\Delta_b}{\omega_m}}(c + c^\dagger)\right] + \frac{1}{2\sqrt{\xi_-}}\left[\beta(b - b^\dagger) + \alpha\sqrt{\frac{\omega_m}{\Delta_b}}(c - c^\dagger)\right]. \tag{B3b}$$

and the inverse:

$$b = \frac{\alpha}{2}\left[\frac{1}{\sqrt{\xi_+}}(d_+ + d_+^\dagger) + \sqrt{\xi_+}(d_+ - d_+^\dagger)\right] + \frac{\beta}{2}\left[\frac{1}{\sqrt{\xi_-}}(d_- + d_-^\dagger) + \sqrt{\xi_-}(d_- - d_-^\dagger)\right], \tag{B4a}$$

$$c = -\frac{\beta}{2}\left[\sqrt{\frac{\omega_m}{\xi_+\Delta_b}}(d_+ + d_+^\dagger) + \sqrt{\frac{\xi_+\Delta_b}{\omega_m}}(d_+ - d_+^\dagger)\right] + \frac{\alpha}{2}\left[\sqrt{\frac{\omega_m}{\xi_-\Delta_b}}(d_- + d_-^\dagger) + \sqrt{\frac{\xi_-\Delta_b}{\omega_m}}(d_- - d_-^\dagger)\right]. \tag{B4b}$$

Now it is straightforward to write the nonlinear interaction in terms of the normal mode coordinates:

$$
\begin{aligned}
H_{\mathrm{nl}} = &-g_0 a^\dagger b(c + c^\dagger) + \mathrm{h.c.} \\
= &-g_0\sqrt{\frac{\omega_m}{\Delta_b}}\left[-\frac{\alpha\beta}{2\xi_+}(a + a^\dagger)(d_+ + d_+^\dagger)^2 + \frac{\alpha\beta}{2}(a - a^\dagger)(d_+^2 - d_+^{\dagger 2})\right. \\
&+\frac{\alpha^2 - \beta^2}{2\sqrt{\xi_+\xi_-}}(a + a^\dagger)(d_+ + d_+^\dagger)(d_- + d_-^\dagger) + \frac{\beta^2}{2}\sqrt{\frac{\xi_-}{\xi_+}}(a - a^\dagger)(d_+ + d_+^\dagger)(d_- - d_-^\dagger) \\
&\left.-\frac{\alpha^2}{2}\sqrt{\frac{\xi_+}{\xi_-}}(a - a^\dagger)(d_- + d_-^\dagger)(d_+ - d_+^\dagger) + \frac{\alpha\beta}{2\xi_-}(a + a^\dagger)(d_- + d_-^\dagger)^2 - \frac{\alpha\beta}{2}(a - a^\dagger)(d_-^2 - d_-^{\dagger 2})\right].
\end{aligned}
\tag{B5}
$$

We now look at the simplified expressions of the normal mode operators and the nonlinear interaction hamiltonian in the regimes of interest. Define $\tan\phi = \dfrac{\omega_m}{\Delta_b}$, $r = 2\dfrac{G_0}{\omega_m}\sqrt{\dfrac{\omega_m}{\Delta_b}}$ and $\alpha = \cos\theta$, $\beta = \sin\theta$, then the diagonalization condition reduces to

$$
\tan 2\theta = r\tan 2\phi,
\tag{B6}
$$

and the normal mode energies become

$$
\xi_\pm^2 = \frac{1}{2}(1 + \tan^2\phi)\left(1 \pm \sqrt{\cos^2 2\phi + r^2\sin^2 2\phi}\right).
\tag{B7}
$$

We now consider the regime where the mechanical frequency is small compared to the detuning of mode b and the driving is so strong that r is close to 1. This allows us to introduce two small parameters $\eta \equiv \omega_m/\Delta_b$ and $\zeta \equiv \sqrt{1 - r^2}$. When $\eta \ll 1$, $\tan\phi \approx \sin\phi \ll 1$, and we have

$$
\xi_+ \approx 1 + r^2\omega_m^2/2\Delta_b^2 = 1 + r^2\eta^2/2,
\tag{B8a}
$$

$$
\xi_- \approx \sqrt{1 - r^2}\,\omega_m/\Delta_b = \zeta\eta.
\tag{B8b}
$$

The diagonalized hamiltonian becomes:

$$
H_0 = \Delta_a a^\dagger a + (\Delta_b + \delta)\bar{b}^\dagger\bar{b} + \omega_m\zeta d^\dagger d,
\tag{B9}
$$

with $\delta = r^2\omega_m\eta/2$ and the new notations for the normal modes are defined as:

$$
\bar{b} \equiv d_+ \approx b - \frac{r}{2}\sqrt{\eta}(c + c^\dagger),
\tag{B10a}
$$

$$
d \equiv d_- \approx \frac{1}{2\sqrt{\zeta}}(c - c^\dagger) + \frac{\sqrt{\zeta}}{2}(c + c^\dagger) + \frac{r}{2}\sqrt{\frac{\eta}{\zeta}}(b - b^\dagger).
\tag{B10b}
$$

The full hamiltonian, including the nonlinear terms, is thus given by Eq. (6).

Appendix C: Derivation of $g^2(0)$ when quantum jumps are neglected

Here we show the standard procedure for calculating the two-photon correlation function $g^2(0)$ in the quasi-steady state regime using an effective hamiltonian. We consider the hamiltonian Eq. (1) (in the main text) with antihermitian terms describing the dissipation and weak coherent probe field on the $\bar{b}$ mode at frequency $\omega_p = \Delta_{\bar{b}} - g_{\mathrm{nl}}$:

$$
\begin{aligned}
H_{\mathrm{eff}} = &(\Delta_a - i\kappa/2)a^\dagger a + (\Delta_{\bar{b}} - i\kappa/2)\bar{b}^\dagger\bar{b} + \omega_m\zeta d^\dagger d \\
&- g_{\mathrm{nl}}(a^\dagger\bar{b} + \bar{b}^\dagger a)(d + d^\dagger) + i\beta_{\bar{b}}(\bar{b}^\dagger e^{-i\omega_p t} - \bar{b}e^{i\omega_p t}).
\end{aligned}
\tag{C1}
$$

The term $(a + a^\dagger)(d^2 + d^{\dagger 2} + 2d^\dagger d)$ has been neglected since its strength is weak in the limit $\Delta_b \gg \omega_m$ and it is also far off resonant. Moving to a frame rotating at ω_p for the optical fields and using the resonance condition $\Delta_{\bar{b}} = \Delta_a + \omega_m\zeta$, we get

$$
\begin{aligned}
H_{\mathrm{eff}} = &(-\omega_m\zeta - i\kappa/2)a^\dagger a + (g_{\mathrm{nl}} - i\kappa/2)\bar{b}^\dagger\bar{b} + \omega_m\zeta d^\dagger d \\
&- g_{\mathrm{nl}}(a^\dagger\bar{b} + \bar{b}^\dagger a)(d + d^\dagger) + i\beta_{\bar{b}}(\bar{b}^\dagger - \bar{b}).
\end{aligned}
\tag{C2}
$$

The system evolves according to the effective hamiltonian and we can expand its quasi-steady state in the following basis:

$$
\begin{aligned}
|\psi\rangle_{\mathrm{ss}} = &|0,0,0\rangle + c_1|0,1,0\rangle + c_2|1,0,1\rangle + c_3|0,1,2\rangle \\
&+ c_4|0,2,0\rangle + c_5|1,1,1\rangle + c_6|2,0,2\rangle + c_7|0,2,2\rangle \\
&+ c_8|200\rangle.
\end{aligned}
\tag{C3}
$$

Considering the following coupling between basis states

$$
|0,1,0\rangle \xleftrightarrow{g_{\mathrm{nl}}} |1,0,1\rangle \xleftrightarrow{\sqrt{2}g_{\mathrm{nl}}} |0,1,2\rangle
$$

$$
|0,2,0\rangle \xleftrightarrow{\sqrt{2}g_{\mathrm{nl}}} |1,1,1\rangle \xleftrightarrow{2g_{\mathrm{nl}}} |2,0,2\rangle
$$

$$
\xleftrightarrow{2g_{\mathrm{nl}}} |0,2,2\rangle
$$

$$
\xleftrightarrow{\sqrt{2}g_{\mathrm{nl}}} |2,0,0\rangle
$$

and the pumping processes

$$
|0,0,0\rangle \xleftrightarrow{\pm i\beta_{\bar{b}}} |0,1,0\rangle \xleftrightarrow{\pm i\beta} |0,2,0\rangle
$$

$$
|1,0,1\rangle \xleftrightarrow{\pm i\beta_{\bar{b}}} |1,1,1\rangle
$$

$$
|0,1,2\rangle \xleftrightarrow{\pm i\beta_{\bar{b}}} |0,2,2\rangle,
$$

we can then construct the matrix representation of the effective hamiltonian.

The steady state is found using the Schrödinger equation:

$$0 = i\frac{\partial}{\partial t}\left|\psi\right\rangle_{\mathrm{ss}} = H_{\mathrm{eff}}\left|\psi\right\rangle_{\mathrm{ss}}. \qquad \text{(C4)}$$

Solving this set of algebra equations gives us the steady state $\left|\psi\right\rangle_{\mathrm{ss}}$. The $g^2(0)$ is calculated using Eq. (13) (main text) in the limit $\beta_{\bar{b}} \to 0$.

[1] G. J. Milburn, Phys. Rev. Lett. **62**, 2124 (1989).
[2] Q. A. Turchette, C. J. Hood, W. Lange, H. Mabuchi, and H. J. Kimble, Phys. Rev. Lett. **75**, 4710 (1995).
[3] H. J. Caulfield and S. Dolev, Nature Photon. **4**, 261 (2010).
[4] J. L. O'Brien, A. Furusawa, and J. Vučković, Nature Photon. **3**, 687 (2009).
[5] K. M. Birnbaum, A. Boca, R. Miller, A. D. Boozer, T. E. Northup, and H. J. Kimble, Nature **436**, 87 (2005).
[6] D. Press, S. Götzinger, S. Reitzenstein, C. Hofmann, A. Löffler, M. Kamp, A. Forchel, and Y. Yamamoto, Phys. Rev. Lett. **98**, 117402 (2007).
[7] L. S. Bishop, J. M. Chow, J. Koch, A. A. Houck, M. H. Devoret, E. Thuneberg, S. M. Girvin, and R. J. Schoelkopf, Nature Phys. **5**, 105 (2009).
[8] T. Volz, A. Reinhard, M. Winger, A. Badolato, K. J. Hennessy, and E. L. Hu, Nature Photon. **6**, 605 (2012).
[9] R. Bose, D. Sridharan, H. Kim, G. S. Solomon, and E. Waks, Phys. Rev. Lett. **108**, 227402 (2012).
[10] W. Chen, K. M. Beck, R. Bücker, M. Gullans, M. D. Lukin, H. Tanji-Suzuki, and V. Vuletić, Science **341**, 768 (2013).
[11] A. Reiserer, N. Kalb, G. Rempe, and S. Ritter, Nature **508**, 237 (2014).
[12] T. G. Tiecke, J. D. Thompson, N. P. de Leon, L. R. Liu, V. Vuletic, and M. D. Lukin, Nature **508**, 241 (2014).
[13] A. Imamoglu, H. Schmidt, G. Woods, and M. Deutsch, Phys. Rev. Lett. **79**, 1467 (1997).
[14] M. D. Lukin and A. Imamoglu, Phys. Rev. Lett. **84**, 1419 (2000).
[15] C.-C. Lin, M.-C. Wu, B.-W. Shiau, Y.-H. Chen, I. A. Yu, Y.-F. Chen, and Y.-C. Chen, Phys. Rev. A **86**, 063836 (2012).
[16] J. Hwang, M. Pototschnig, R. Lettow, G. Zumofen, A. Renn, S. Götzinger, and V. Sandoghdar, Nature **460**, 76 (2009).
[17] T. Peyronel, O. Firstenberg, Q.-Y. Liang, S. Hofferberth, A. V. Gorshkov, T. Pohl, M. D. Lukin, and V. Vuletić, Nature **488**, 57 (2012).
[18] Y. O. Dudin and A. Kuzmich, Science **336**, 887 (2012).
[19] H. Gorniaczyk, J. S. C. Tresp, H. Fedder, and S. Hofferberth, (2014), arXiv:1404.2876.
[20] D. Tiarks, S. Baur, K. Schneider, S. Dürr, and G. Rempe, (2014), arXiv:1404.3061.
[21] D. E. Chang, A. S. Sørensen, E. A. Demler, and M. D. Lukin, Nature Phys. **3**, 807 (2007).
[22] M. Gullans, D. E. Chang, F. H. L. Koppens, F. J. García de Abajo, and M. D. Lukin, Phys. Rev. Lett. **111**, 247401 (2013).
[23] M. Bajcsy, S. Hofferberth, V. Balic, T. Peyronel, M. Hafezi, A. S. Zibrov, V. Vuletic, and M. D. Lukin, Phys. Rev. Lett. **102**, 203902 (2009).
[24] V. Venkataraman, K. Saha, P. Londero, and A. L. Gaeta, Phys. Rev. Lett. **107**, 193902 (2011).
[25] P. Kolchin, R. F. Oulton, and X. Zhang, Phys. Rev. Lett. **106**, 113601 (2011).
[26] D. O'Shea, C. Junge, J. Volz, and A. Rauschenbeutel, Phys. Rev. Lett. **111**, 193601 (2013).
[27] T. J. Kippenberg and K. J. Vahala, Science **321**, 1172 (2008).
[28] M. Aspelmeyer, T. J. Kippenberg, and F. Marquardt, (2013), arXiv:1303.0733.
[29] J. D. Thompson, B. M. Zwickl, A. M. Jayich, F. Marquardt, S. M. Girvin, and J. G. E. Harris, Nature **452**, 72 (2008).
[30] J. Chan, T. P. M. Alegre, A. H. Safavi-Naeini, J. T. Hill, A. Krause, S. Gröblacher, M. Aspelmeyer, and O. Painter, Nature **478**, 89 (2011).
[31] E. Verhagen, S. Delglise, S. Weis, A. Schliesser, and T. J. Kippenberg, Nature **482**, 63 (2012).
[32] S. Gröblacher, K. Hammerer, M. R. Vanner, and M. Aspelmeyer, Nature **460**, 724 (2009).
[33] J. D. Teufel, D. Li, M. S. Allman, K. Cicak, A. J. Sirois, J. D. Whittaker, and R. W. Simmonds, Nature **471**, 204 (2011).
[34] M.-A. Lemonde, N. Didier, and A. A. Clerk, Phys. Rev. Lett. **111**, 053602 (2013).
[35] K. Børkje, A. Nunnenkamp, J. D. Teufel, and S. M. Girvin, Phys. Rev. Lett. **111**, 053603 (2013).
[36] A. Kronwald and F. Marquardt, Phys. Rev. Lett. **111**, 133601 (2013).
[37] P. Rabl, Phys. Rev. Lett. **107**, 063601 (2011).
[38] A. Nunnenkamp, K. Børkje, and S. M. Girvin, Phys. Rev. Lett. **107**, 063602 (2011).
[39] J. Qian, A. A. Clerk, K. Hammerer, and F. Marquardt, Phys. Rev. Lett. **109**, 253601 (2012).
[40] P. Kómár, S. D. Bennett, K. Stannigel, S. J. M. Habraken, P. Rabl, P. Zoller, and M. D. Lukin, Phys. Rev. A **87**, 013839 (2013).
[41] X.-Y. Lu, W.-M. Zhang, S. Ashhab, Y. Wu, and F. Nori, Sci. Rep. **3**, 2943 (2013).
[42] X. Xu and J. M. Taylor, Phys. Rev. A **90**, 043848 (2014).
[43] Supplementary material contains the derivation of the full normal mode Hamiltonian and the derivation of the minimum $g^{(2)}(0)$ when quantum jumps are neglected.
[44] J. Chan, M. Eichenfield, R. Camacho, and O. Painter, Opt. Express **17**, 3802 (2009).
[45] J. Chan, A. H. Safavi-Naeini, J. T. Hill, S. Meenehan, and O. Painter, Applied Physics Letters **101**, 081115 (2012).
[46] J. Gomis-Bresco, D. Navarro-Urrios, M. Oudich, S. El-Jallal, A. Griol, D. Puerto, E. Chavez, Y. Pennec, B. Djafari-Rouhani, F. Alzina, A. Martnez, and C. S. Torres, Nat Commun **5**, 4452 (2014).
[47] A. H. Safavi-Naeini, J. T. Hill, S. Meenehan, J. Chan, S. Gröblacher, and O. Painter, Phys. Rev. Lett. **112**, 153603 (2014).
[48] H. Sekoguchi, Y. Takahashi, T. Asano, and S. Noda, Opt. Express **22**, 916 (2014).